Chapter 2

Concepts for Regasification of LNG in Industrial Parks

Tatiana Morosuk, Stefanie Tesch and

George Tsatsaronis

Additional information is available at the end of the chapter

http://dx.doi.org/10.5772/intechopen.70118

Abstract

The exponentially growing markets of liquefied natural gas (LNG) require efficient processes for LNG regasification within import terminals. Usually, the regasification of LNG is accomplished by direct or indirect heating. However, integrating LNG regasification into different processes within industrial parks (mainly processes involving low temperatures) is an efficient approach because of the utilization of the low-temperature energy. In some LNG import terminals, integration technologies are already being used. Previous publications showed an increase in the thermodynamic efficiency for systems combining air separation (as an example) and LNG regasification. In addition, the variation in the efficiency as well as the capital investment depends on the schematic and operation conditions. This fact creates great potential for improving the systems. In this chapter, different schematics are evaluated using exergy-based methods in order to improve the effectiveness of complex industrial processes that can involve LNG regasification.

Keywords: LNG, regasification, refrigeration process, cryogenic process, exergy-based methods

1. Introduction

Natural gas became a very important primary energy carrier in the last decades. The world fuel share of natural gas increased from 16% (in the year 1973) to 21% at present. Approximately 50% of the natural gas is supplied as liquefied natural gas (LNG) (**Figure 1**). In the year 2015, 19 countries exported LNG, with Qatar, Australia, Malaysia, and Nigeria being the main exporting countries. The number of importing countries increased to 34 in the year 2015 [1–4].

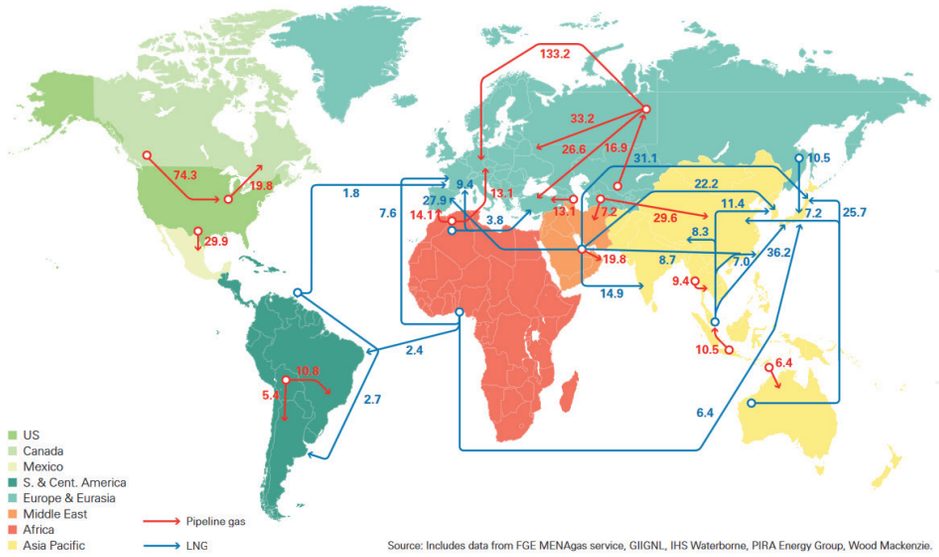

Figure 1. Major trade movements 2015 (in billion cubic meters) [3].

The total chain of LNG consists of the following four steps: exploration and pretreatment, liquefaction and storage, transportation by ship as well as regasification, storage, and distribution.

Figure 2 shows the options of different technologies for the regasification of LNG. Thermal energy coming from the combustion of natural gas, seawater or cooling water, air, and process integration technologies can be used for the regasification of LNG.

A heat transfer process (direct or indirect) between LNG and other working fluid(s) is the basic principle used for the regasification of LNG (**Figure 2a**) in almost all import terminals overall the world. At present, five regasification technologies are used [5]: open rack vaporizers (ORV), shell-and-tube vaporizers (STV), submerged combustion vaporizers (SCV), and combined heat and power units with submerged combustion units (CHP-SCV). Other types of vaporizers, the so-called atmospheric evaporators, are used only for the regasification of very small amounts of LNG and operate periodically. Heat from industrial processes can also be used for the regasification of LNG (**Figure 2b**), and this, however, will not affect the improvement of the industrial process, because the block "regasification of LNG" and block "Industry/Power Plant" have separate system boundaries. Techno-economic evaluation of these options is discussed in Refs. [6, 7]. Within these technologies (**Figure 2a** and **b**), the low-temperature exergy of the LNG is destroyed without any use.

However, low-temperature exergy of the LNG is a valuable "fuel" for many industrial processes such as chemical, power generation, and so on. Therefore, researchers are working on the development of different options for using the low-temperature exergy of LNG (**Figure 2c** and **d**). These options can be classified as "industrial parks" because the vaporization of LNG becomes an integral part of complex processes generating electricity or chemical products (common boundary conditions). There are two options for the realization of the concepts (**Figure 2c** and **d**):

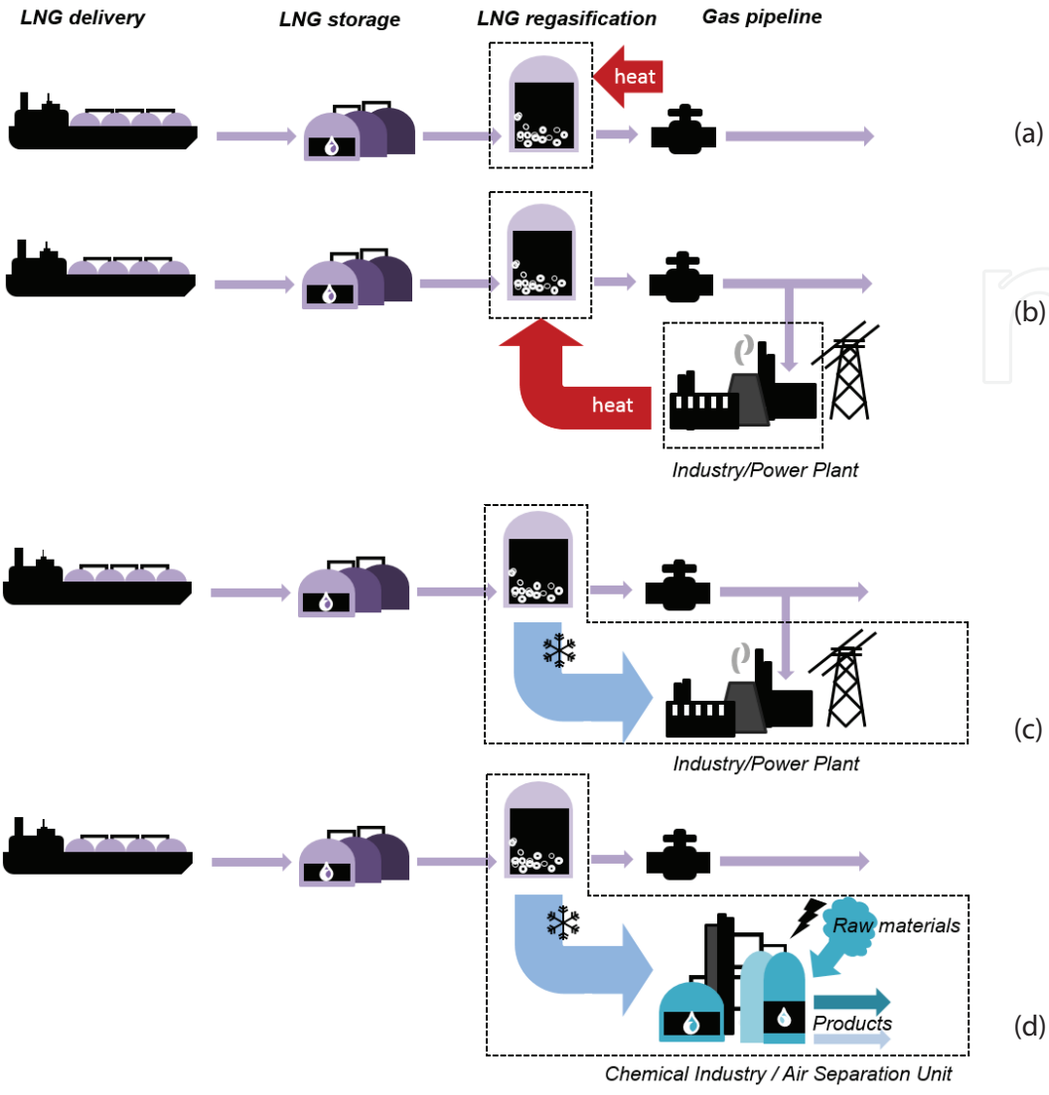

Figure 2. Options for the regasification of LNG: (a) direct or indirect heat transfer process, for example, ORV, STV, and SCV; (b) heat utilization of an industrial process; (c) LNG-based cogeneration for electricity generation; and (d) LNG-based cogeneration for chemical products.

- The regasification of LNG could be integrated into a system for the generation of electricity. One of the first publications, where this idea has been described, was Ref. [8]. An extended review of such technologies as well as novel concepts was reported, for example, in Refs. [9, 10].
- The low-temperature exergy of LNG could be used within: (a) desalination processes as reported in Refs. [11, 12] and (b) agro-industrial processes for freezing purposes as discussed in Refs. [13–15].

The implementation of the regasification of LNG into chemical industries (**Figure 2d**) is well known from the industrial project developed by Osaka Gas in Japan [16]. Here, the LNG import terminal is integrated within an industrial complex with refinery and petrochemical plants. LNG is regasified in four steps, which is related to the temperature levels of the refinery and the petrochemical plant. These steps are as follows: (a) separation of light hydrocarbons

produced as a by-product in the oil refining process (the temperature level is around −100°C; an energy source to separate olefin used as a raw material of polymer products at the petrochemical plant), (b) liquefaction of carbon dioxide, a by-product in the production of hydrogen (the temperature level is around −55°C), (c) low-temperature storage of butane (−8°C), and (d) cooling of water used to cool the intake air for gas turbines (10°C).

Since this chapter focuses on the regasification of LNG in conjunction with air separation processes (concept of industrial parks shown in **Figure 2d**), the state-of-art of such a technology will be given.

A concept for the regasification of LNG integrated into an air separation unit was reported in Ref. [17]. A recycle nitrogen stream is used to evaporate the LNG stream. This integration leads to a decrease in the total specific power consumption from 1.3 kWh/m^3 (related to the sum of oxygen and nitrogen steams) to 0.8 kWh/m^3. In addition to that the installation costs are reduced by 10%.

In Ref. [18] was proposed a high-performance energy-supply system with cryogenic air separation using the cold of LNG and a power generation system with gas and steam turbines, where the required electrical power is reduced from 1.2 kWh/m^3 (per oxygen steam) to 0.57 kWh/m^3. In this paper, two different options of a double-column distillation process are discussed.

The integration of the regasification of LNG into a one-column air separation system was proposed and evaluated in Ref. [19]. The reported power consumption is decreased by 39%. Another configuration of a one-column air separation system with an oxy-fuel power generation cycle and regasification of LNG was evaluated in Ref. [20]. The achieved reduction in the power consumption is 38.5%. Later, a novel system has been developed [21], where the cold of LNG is used to precool the air. The power consumption is decreased in this case by 56%.

There are also several patents related to the integration of LNG into an air separation unit, e.g., Refs. [22–26]. The data related to energy consumption or/and efficiency are not mentioned.

The authors developed several concepts for the integration of LNG regasification into air separation systems. Conventional and advanced exergy analyses as well as economic analyses have been applied to evaluate the performance of these industrial parks. Detailed information can be found in Refs. [27, 28].

2. Process description

Before the authors' concepts for integrating LNG regasification into air separation systems are discussed, a conventional air separation process is evaluated. In this chapter, only generalized information based on Refs. [27, 28] have been reported.

2.1. Case A—air separation unit

Main products of an air separation unit are oxygen and nitrogen, which could be in liquid and in gaseous form. In some air separations plants, noble gases (argon, for example) are gained. The typical air separation unit is composed of three to four blocks:

- Air compression and purification block
- Air liquefaction block (main heat exchanger (MHE))
- Column block (CB)
- Nitrogen liquefaction block (NLB) (is not mandatory).

The nitrogen liquefaction block is necessary in order to produce higher amounts of liquid products and to achieve a higher purity of the products. This block consists of a large number of components. It affects the thermodynamic efficiency and the investment costs. The conceptual design of the single air separation unit (Case A) is shown in **Figure 3**.

2.1.1. Air compression and purification block

The air compression block consists of two air compressors with interstage cooler. The dustless air is compressed to 5.6 bar [29]. Within the purification block, impurities which will freeze at low temperatures are removed using adsorption technology. The considered impurities in the compressed air stream are water vapor and carbon dioxide. The concentration must be lower than 0.1 ppm for water vapor and 1.0 ppm for carbon dioxide [30].

2.1.2. Main heat exchanger

The compressed air leaving the air compression and purification block is cooled to −173 °C within the MHE. The air leaves the MHE partially in liquid form. The streams leaving the column block are used to cool down the air. The MHE is a multi-stream (four cold and one hot stream) counterflow heat exchanger and is together with the column block embedded in a so-called cold box in order to decrease the heat sink from the environment.

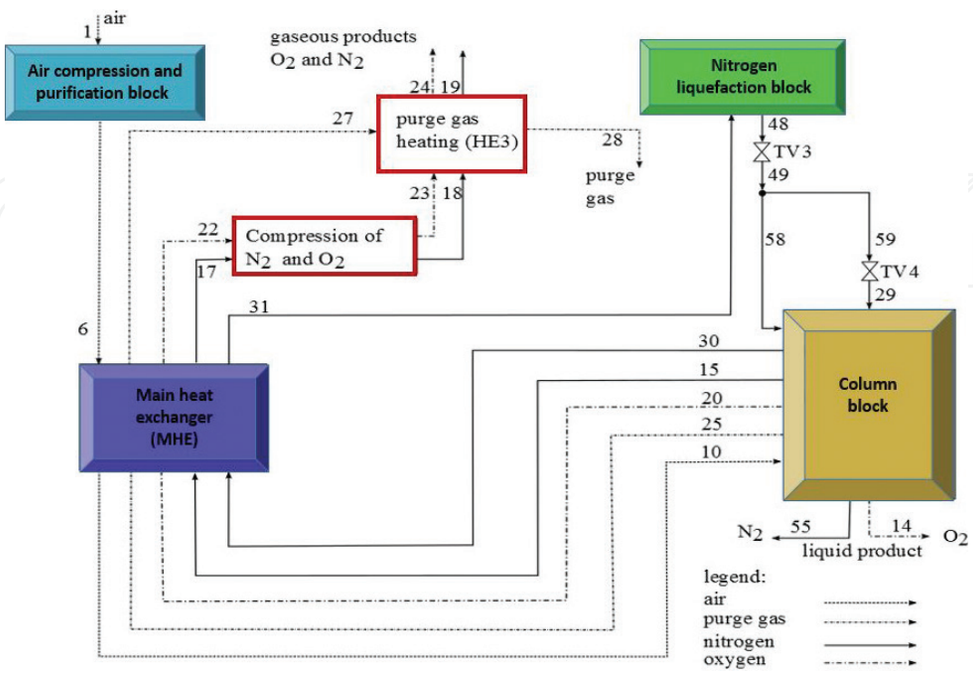

Figure 3. Conceptual schematic of Case A (air separation unit).

2.1.3. Column block

After the MHE, the cold air is fed to the column block. The column block consists of two separate columns, which are thermally coupled by the condenser/reboiler. The lower column is the high-pressure column (HPC), with a pressure of 5.6 bar, and the upper column is the low-pressure column (LPC) with a pressure of 1.3 bar. Both columns are simulated as sieve tray columns. Several side streams leaving the HPC are fed to the LPC. The top-products of the HPC are gaseous and liquid nitrogen streams. The liquid nitrogen stream is removed from the system as a product stream, and the gaseous stream is fed to the MHE. The top product of the LPC is also gaseous nitrogen, which is fed to the MHE. At the bottom, liquid and gaseous oxygen are gained. While the liquid stream is also removed from the system, the gaseous stream is fed to the MHE. In addition, a side stream from the LPC is fed to the MHE which contains mainly nitrogen and is called purge gas stream.

2.1.4. Nitrogen liquefaction block

The NLB consists of four compressors, two expanders, two heat exchangers, and several mixing and splitting devices [27]. One of the two gaseous nitrogen streams (stream 31) within the MHE is fed to the nitrogen liquefaction block. Here, stream 31 is mixed with streams 44 and 47, which are already in the nitrogen liquefaction block. The resulting stream (stream 32) is then heated in HE1 and compressed within a three-stage compression process with interstage cooling to 38 bar. The stream is split into streams 45 and 39. Stream 39 is fed to NC4, compressed to 46 bar, and fed together with stream 45 to HE1, where both streams are cooled. The stream with a pressure of 38 bar (stream 46) is afterwards fed to EXP1 and mixed with the incoming stream. The second stream leaving the HE1 is again split into two streams: stream 42 and stream 21. Stream 42 is fed to EXP2, and after this, it is used in the HE2 to cool stream 21. This stream leaves the nitrogen liquefaction block (stream 48) and is split into two parts (streams 58 and 59), which are fed to both columns as a reflux.

2.1.5. Product compression

The nitrogen and oxygen streams leaving the MHE are fed to the NC5 and OC and are compressed to 20 bar, but this pressure depends on the consumer. After compression, the nitrogen stream is used to heat the purge gas stream, which also leaves the MHE. The required temperature for the purge gas is 170°C [31], because the purge gas stream is used to desorb the impurities in the purification block.

2.2. Case A Design 1

Case A Design 1 (Case AD 1) (**Figure 4** [27]) is the concept of the industrial park where the LNG stream is regasified within the MHE after having been pressurized in an LNG pump.

The air compression and purification block is identical with the same block in Case A.

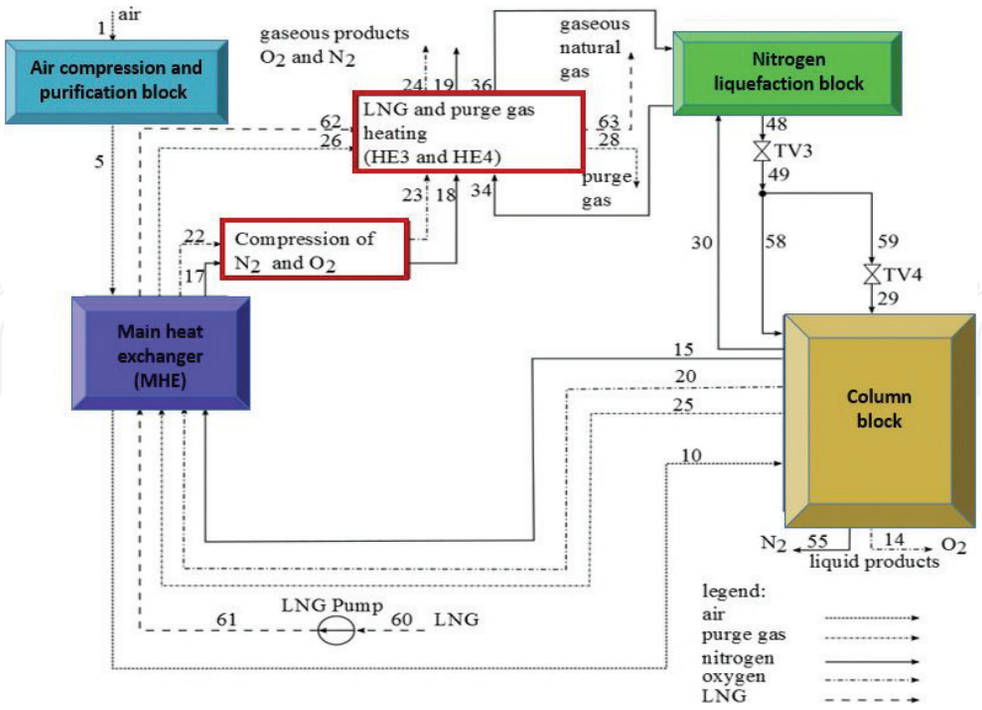

Figure 4. Conceptual schematic of Case AD1.

2.2.1. Main heat exchanger

In comparison to Case A, the main heat exchanger is adjusted by the LNG stream. It also includes four cold streams, which are now oxygen, purge gas, nitrogen, and LNG (the second nitrogen stream is not used within the MHE anymore). The hot stream is air, which is cooled to −173 °C.

2.2.2. Column block

The column block is almost identical to the column block in Case A. The only difference is that the top product (nitrogen stream, stream 30) is directly fed to the nitrogen liquefaction block, instead of passing by the MHE.

2.2.3. Nitrogen liquefaction block

The implementation of LNG within MHE has affected the nitrogen liquefaction block. Here, the nitrogen liquefaction block consists of three compressors, one expander, as well as one mixing and one splitting device. The top product of the HPC (stream 30) is fed to the NLB, heated in the HE2, and afterwards mixed with stream 44, which is also heated in the HE2 (stream 42). They form stream 32, which is heated in the HE1 and is then compressed in a three-stage compression process. Between the first and the second stages, the stream is cooled in HE3, which is located in the product compression block. After the compression process, the stream is cooled in HE1 and split into streams 42 and 41. Stream 42 is fed to EXP2, heated

within HE2, and mixed with the incoming stream 30, whereas stream 41 is cooled within the HE2 and fed to the column block as a reflux.

2.2.4. Product compression

Also in this system, the product streams are compressed to 20 bar. One more heat exchanger is required here in comparison with Case A. Here, the nitrogen stream from the NLB is used to heat the purge gas stream to the required temperature (HE3). This nitrogen stream and the nitrogen stream leaving the NC5 are fed to the HE4 in order to heat the LNG stream to ambient temperature.

2.3. Case A Design 2

Case A Design 2 (Case AD2) (**Figure 5** [27]) is the concept where LNG being pressurized in an LNG pump is further regasified within MHE, the air compression and purification block, and the nitrogen liquefaction block. The concept is shown in **Figure 5**.

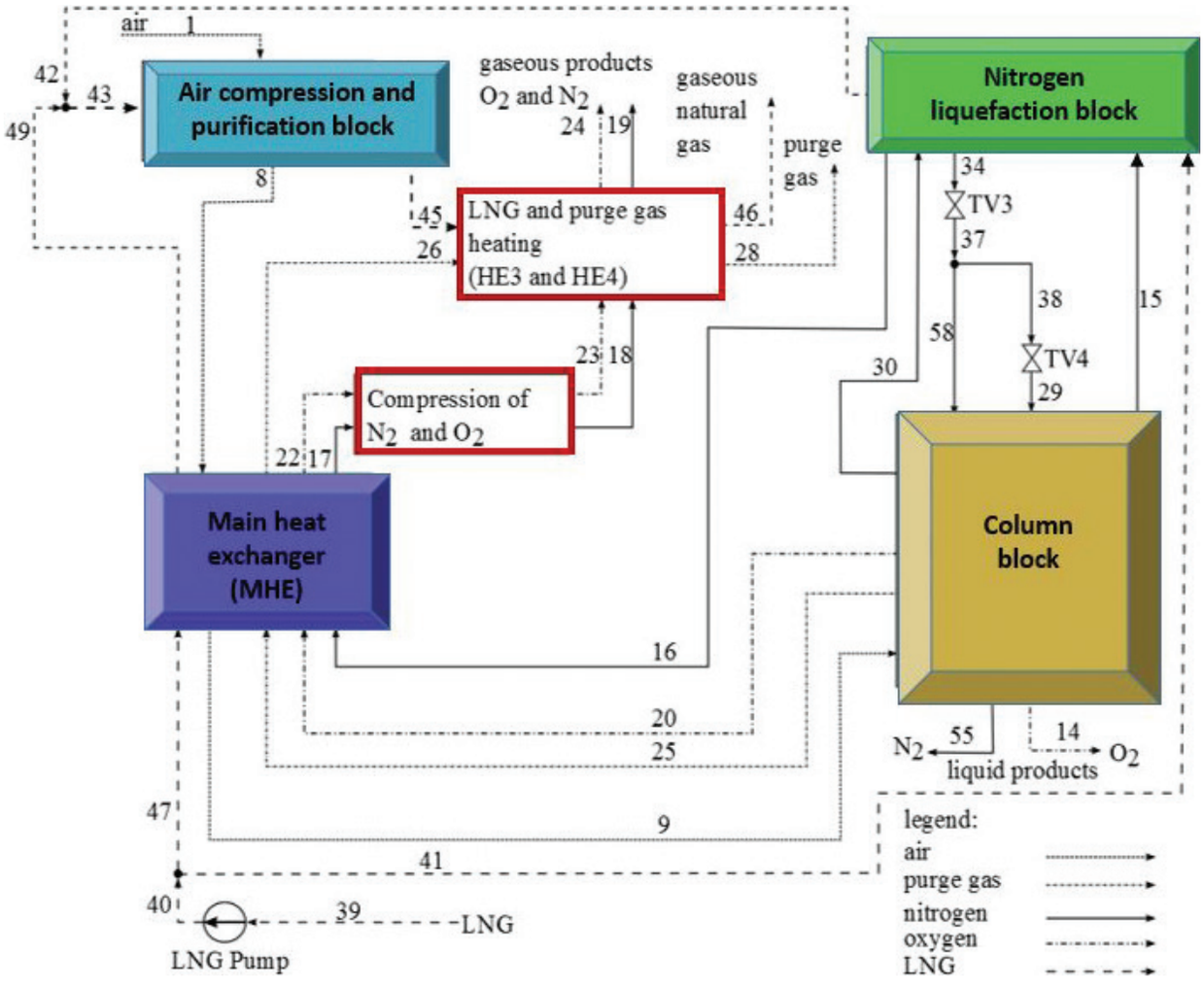

Figure 5. Conceptual schematic of Case AD2.

2.3.1. Air compression and purification block

The structure of the air compression and purification block differs from the structure of the two systems discussed above. In Case AD2, air is compressed within a three-stage compression processes to 5.6 bar, which requires an additional interstage cooler. The cooling medium in the interstage coolers is the LNG stream. Thus, after the water has been removed from the air, the air could be cooled to a lower temperature while heating the LNG stream. This leads to a decrease in the power consumption in the following air compressors. Consequently, the air enters the MHE with a slightly lower temperature compared to Cases A and AD1.

2.3.2. Main heat exchanger

The main heat exchanger has the same structure as in Case AD1. The cold streams are gaseous oxygen, nitrogen, purge gas, and the LNG, whereas the hot stream is air. Hence, in Case AD2, the LNG stream is divided into two parts: one is fed to the MHE, and the second one to the nitrogen liquefaction block.

2.3.3. Column block

The column block is identical to the Case AD1. In addition, here the top-product of the LPC is directly fed to the nitrogen liquefaction block.

2.3.4. Nitrogen liquefaction block

The structure of the nitrogen liquefaction is different from the Cases A and AD1. It now consists of only one heat exchanger and two compressors. The top product of the HPC (stream 30) and one part of the total LNG stream are heated in the HE2. The nitrogen stream is compressed within a two-stage compression process. Afterwards, it is cooled in the HE2 and fed to both columns as a reflux.

2.3.5. Product compression

The gaseous oxygen and nitrogen streams leaving the MHE are also compressed to 20 bar. The nitrogen stream is then used to heat the purge gas. Finally, the LNG stream is heated to ambient temperature within HE4 using the compressed nitrogen and oxygen streams and the heated pure gas stream.

3. Methodology

The exergy-based methods are meaningful tools to analyze, understand, and improve energy conversion systems [32]. These methods consist of several analyses [33, 34]:

- Conventional exergy analysis
- Exergoeconomic analysis

- Exergoenvironmental analysis
- Advanced exergy analysis
- Advanced exergoeconomic analysis
- Advanced exergoenvironmental analysis.

In this chapter, the conventional and advanced exergetic analyses are applied for evaluation of the three proposed cases. Additionally, the results from an economic analysis are reported.

3.1. Conventional exergetic analysis

A conventional exergetic analysis identifies the sources of the thermodynamic inefficiencies within components and the overall system. The approaches "exergy of fuel" and "exergy of product" are applied [32]. The exergy destruction within each component (Eq. (1), the subscript *k* refers to the component being evaluated) and within the overall system (Eq. (2), subscript *tot*) is calculated from

$$\dot{E}_{\mathrm{F,k}} = \dot{E}_{P,\mathrm{k}} + \dot{E}_{D,\mathrm{k}} \tag{1}$$

$$\dot{E}_{\mathrm{F,tot}} = \dot{E}_{P,\mathrm{tot}} + \dot{E}_{D,\mathrm{tot}} + \dot{E}_{L,\mathrm{tot}} \tag{2}$$

The exergetic efficiencies of component *k* (Eq. (3a)) and the overall system (Eq. (3b)) are defined as

$$\varepsilon_k = \frac{\dot{E}_{P,\mathrm{k}}}{\dot{E}_{\mathrm{F,k}}} \tag{3a}$$

$$\varepsilon_{tot} = \frac{\dot{E}_{P,\mathrm{tot}}}{\dot{E}_{\mathrm{F,tot}}} \tag{3b}$$

3.2. Advanced exergetic analysis

The advanced exergetic analysis is an extension of the conventional exergy analysis and helps to identify the interrelations among the exergy destructions within the components and the real potential for improving the energy conversion system (the methodology could be found in Refs. [33, 34]. In the advanced exergetic analysis, the exergy destruction could be spilt into avoidable and unavoidable or/and endogenous and exogenous parts. Furthermore, these parts could be combined to determine the

- unavoidable endogenous exergy destruction,
- unavoidable exogenous exergy destruction,
- avoidable endogenous exergy destruction, and
- avoidable exogenous exergy destruction.

The unavoidable exergy destruction represents the part which could not be reduced due to technological limitations associated with the component being considered. Thus, the avoidable exergy destruction is the part which could be reduced by thermodynamically improving the component. The endogenous exergy destruction represents the part which is caused by the irreversibilities within the component itself, while the exogenous exergy destruction is the part which occurs within this component due to the exergy destructions within the remaining components of the overall system.

In this chapter, the exergy destruction is split into unavoidable and avoidable parts. More information about other options to split the exergy destruction has already been reported in Ref. [27].

Splitting the exergy destruction into the unavoidable and avoidable parts requires identifying the technological limitations of the different types of components. The following assumptions are used: minimum temperature difference of 0.5 K for all heat exchangers; maximum isentropic efficiency of 80% for the LNG pump, and maximum isentropic efficiency of 90% for the compressors and expanders. The splitting of the exergy destruction was not applied to the column block, throttling valves, splitting devices, and dissipative components.

3.3. Economic analysis

The economic analysis estimates the cost of components as well as the fixed and total capital investment. In this chapter, the economic analysis is conducted based on Ref. [32]. Additional details are given in Ref. [28].

3.3.1. Purchased equipment costs

The cost of all components (purchased equipment costs (PEC)) is estimated using cost data available in the literature and are adjusted according to the operation conditions using temperature, pressure, and material factors. The factors are obtained from Ref [38], whereby the temperature factor has to be adjusted for temperatures below 0°C. All components which work at temperatures higher than −29°C are made of carbon steel [35]. For lower temperatures, materials like stainless steel, aluminum, cooper, or monel could also be used.

3.3.2. Cost of the heat exchangers

For the heat exchangers, two different kinds of heat exchangers are assumed: shell-and-tube and plate heat exchangers.

The interstage coolers in the air compression and purification block and in the nitrogen liquefaction block are shell-and-tube heat exchangers. The remaining heat exchangers (HE1, HE2, HE3, HE4, and MHE) are plate heat exchangers. To estimate the costs, the heat duty and the temperature differences are obtained from AspenPlus [36]. The overall heat transfer coefficients are selected according to the available data. The costs are estimated based on data from Ref. [37].

3.3.3. Cost of the turbomachinery

This set of components includes the compressor, expanders, and the LNG pump. The compressors are centrifugal compressors and the expanders are axial expanders. For all turbomachinery, the required or generated power is the determined factor for the cost estimation. The costs are taken from Refs. [37–39], for the compressors, expanders, and the pump, respectively.

In general, the cost of compressors includes the cost for the electrical motor. However, in Case A, there is one exception. The cost of NC3 and NC4 is estimated without motor, because they are connected to EXP1 and EXP2, respectively.

3.3.4. Cost of the column block

The estimation of the costs of the column block is divided into two parts: empty shell and trays [29]. The low-pressure and high-pressure columns are simulated as sieve tray columns with 96 and 54 stages, respectively. To estimate the costs of the two empty shells, the diameter and the height must be known. According to Ref. [40], the diameter must be lower than 4–5 m, because, otherwise, it will be difficult and costly to construct a sieve tray column. Here, a diameter of 3 m for both columns is assumed. For the calculation of the height of each column, the distance between each tray must be known. In Refs. [41–43], values of 80 mm to 300 mm, 300 mm to 600 mm, and around 610 mm are mentioned, respectively. We assumed a value of 400 mm, which results in a height of 21.6 m and 38.4 m for the HPC and LPC, respectively. Both columns on top of each other have a total height of 60 m, which is in the range of the size for the cold box of an air separation unit [41]. The estimation of the costs of the trays depends on the diameter of the columns and on the number of trays. The costs for the empty shell and the trays are obtained from data reported in Ref. [39].

3.3.5. Estimation of the costs of the purification system

The estimation of the costs of the purification systems is based on the results of the above-mentioned groups of components. The percentage distribution of the costs of the different types of components is given by Ref. [45]. The purification system accounts for 13% of the total cost of the components.

3.3.6. Fixed and total capital investment costs

After estimation of the purchased equipment costs, the fixed capital investment (FCI) is calculated. The fixed capital investment is the sum of the direct and indirect costs. The direct costs could be further divided into onsite and offsite costs. Here, the offsite costs are here neglected. The onsite costs contain the purchased equipment costs and additional costs such as installation, piping, electrical equipment and instrumentation and controls. In the literature [32, 39], these additional costs are calculated as a share of the purchased equipment costs. Another possibility to consider the additional costs of each component is the modular method, which considers the module factor according to Ref. [44]. Therefore, the purchased equipment cost of each component is multiplied by a specified module factor which is individual for each component type.

The indirect costs consist of engineering, supervision, construction costs, contractor's profit, and contingencies. All these costs are calculated as a given percentage of the direct costs. For the total capital investment (TCI), the different time points of the investments are considered and the related required payments of interest.

3.4. Safety aspects

LNG has an outstanding safety history. Commercial LNG transportation started in the 1960s without serious accidents. Only six incidents which are mainly related to collisions with other ships or run a ground have been reported in Ref. [46], but in all these cases no LNG was released. The good safety history is attributed to the well-developed technology for LNG tankers and the strict safety regulations. Nowadays, two types of LNG carriers exist: spherical type and membrane type. Both tanks are of double-hulled construction, which increases the safety of LNG carriers. Especially since 1980, the number of annual incidents related to the transport of oil, LNG, and LPG decreased due to a wide range of safety regulations, design, crew competence, and ship management improvements [47].

In general, the main hazards related to LNG are fires, explosion, cryogenic freeze burns, embrittlement of metal, and confined spaces [5]. The main sources of LNG hazards are, for example, liquid leaks under pressure, liquid leaks from storage tanks, rollover of an LNG storage tank, and liquid pools evaporating to form a flammable vapor plume [46]. Not all of the above-mentioned sources of LNG hazards occur in each step of the LNG chain. Thus, leaks under pressure occur in liquefaction and regasification process and during the transfer of LNG from storage and vice versa. The risk assessment of the LNG technology is widely spread in the literature. Ramsden et al. [49] published a study including the main important safety regulations for the transport of LNG. A detailed analysis and modelling of the risk associated with LNG was conducted in Ref. [46]. The safety and risk aspects of LNG are also analyzed in Ref. [5].

In case of a spill or leakage of LNG, a fire or explosion is the main hazard related to LNG. The consequences of leaks are shown graphically in a so-called event tree, which is shown in **Figure 6** for a leakage of LNG near atmospheric and at elevated pressure. As shown in this figure, the consequences of spills depend on several facts like type of release, direct or delayed ignition. According to these facts, different kinds of fire occur like pool fire, jet fire, flash fire, or boiling liquid expanding vapor explosion (BLEVE). The presence of pure oxygen or oxygen-enriched streams, low temperatures, and high-pressure streams are associated with the main hazards in air separation plants. In Ref. [48], the following four main hazards are related to air separation units: rapid oxidation, embrittlement, and pressure excursions due to vaporizing liquids and oxygen-enriched or deficient atmospheres. A survey of accidents at Japanese air separation plants conducted [51] and categorized them according to the following types: explosion, burn, frost bite, and suffocation. The component with the highest number of accidents is the reboiler. Mainly, these accidents are explosions due to the accumulation of hydrocarbons within the liquid oxygen.

In the discussed cases with the integration of the LNG regasification, the simultaneous presence of LNG and oxygen increases the hazards potential.

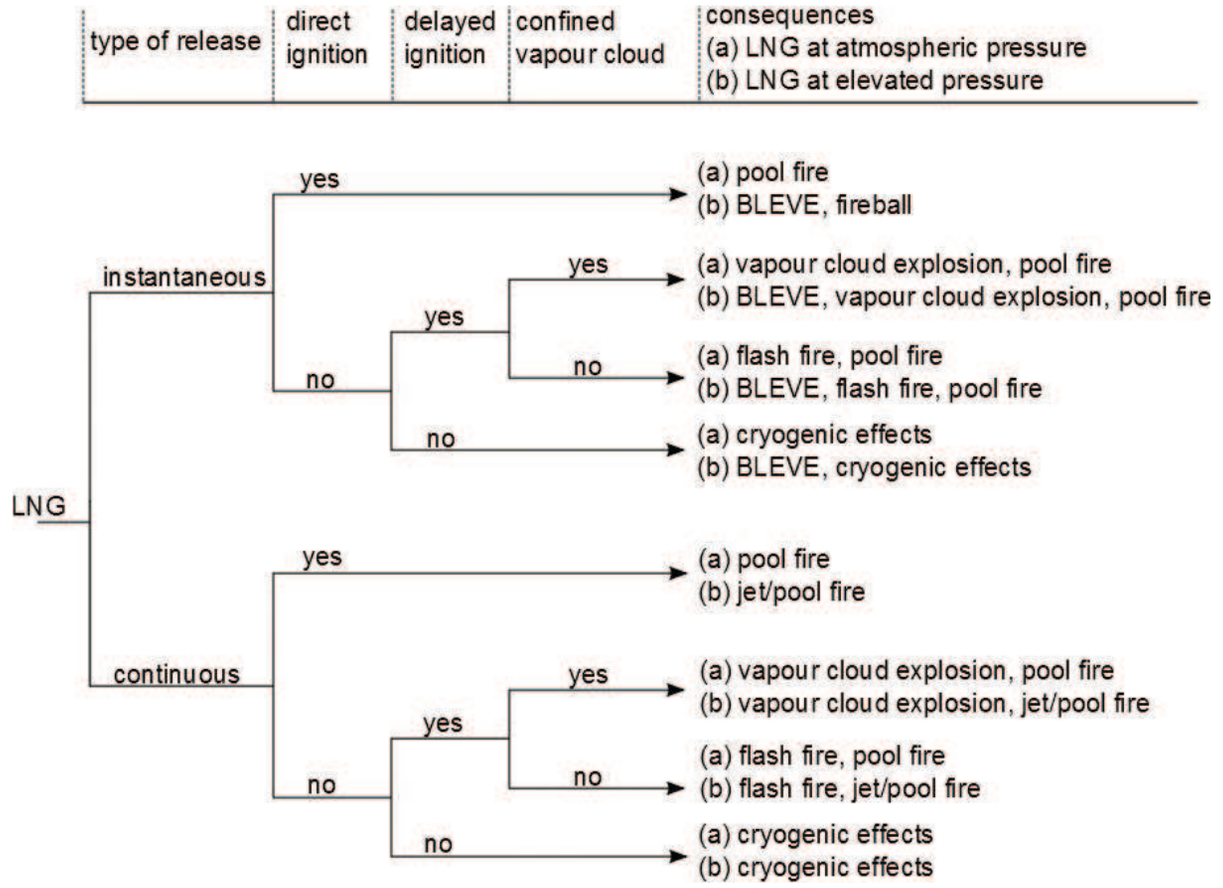

Figure 6. Event tree for the release of LNG at atmospheric and elevated pressure (based on Ref. [49]).

4. Simulation

The simulation of the three discussed cases has been conducted using AspenPlus. The Peng-Robinson equation of state is selected, because it is appropriate for low-temperature processes. **Table 1** shows the assumptions for the two incoming streams: air and LNG. Main assumptions for the simulation of the different types of components are shown in **Table 2**. The detailed description of the simulation is reported in Ref. [27].

Parameters	Unit	Air value	LNG Value
T	°C	15	−162
p	bar	1.0134	1.3
$\dot{m}$	kg/s	16.4	10
x_i	kmol/kmol	$x_{N_2} = 0.772$; $x_{O_2} = 0.208$ $x_{Ar} = 0.0095$; $x_{H_2O} = 0.0102$ $x_{CO_2} = 0.0003$	$x_{CH_4} = 0.8698$; $x_{C_2H_6} = 0.0935$ $x_{C_3H_8} = 0.0233$; $x_{C_4H_{10}} = 0.0063$ $x_{N_2} = 0.0071$

Table 1. Assumptions for the incoming streams.

Parameter	Unit	Value
Compressors, expanders		
η_{is}	–	0.8
η_{mech}	–	0.99
Column block		
Stages (HPC)	–	54
Stages (LPC)	–	96
Stage pressure drop	bar	0.003
Reflux ratio (HPC)	kg/s/kg/s	0.75
Bottom rate (LPC)	kg/s	0.5
Heat exchangers		
Pressure drop	%	3

Table 2. Selected assumptions for different types of components.

5. Results and discussion

5.1. Energy analysis

Figures 7 and **8** show the power consumption/generation within turbomachinery and the heat rate in the heat exchangers, respectively. The total power consumption is $\dot{W}_{tot,CA} = 18.5$ MW for Case A. It decreases to $\dot{W}_{tot,CAD1} = 12.0$ MW and $\dot{W}_{tot,CAD2} = 6.9$ MW, which corresponds to a reduction in the power consumption of 35.2% (Case AD1) and 62.8% (Case AD2).

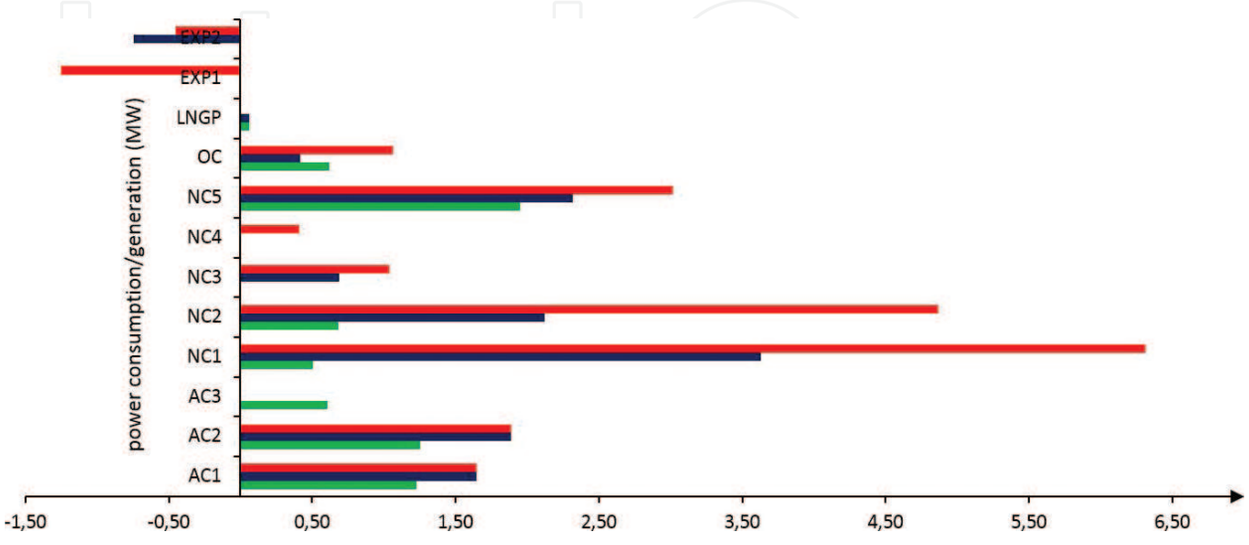

Figure 7. Power consumption/generation (MW).

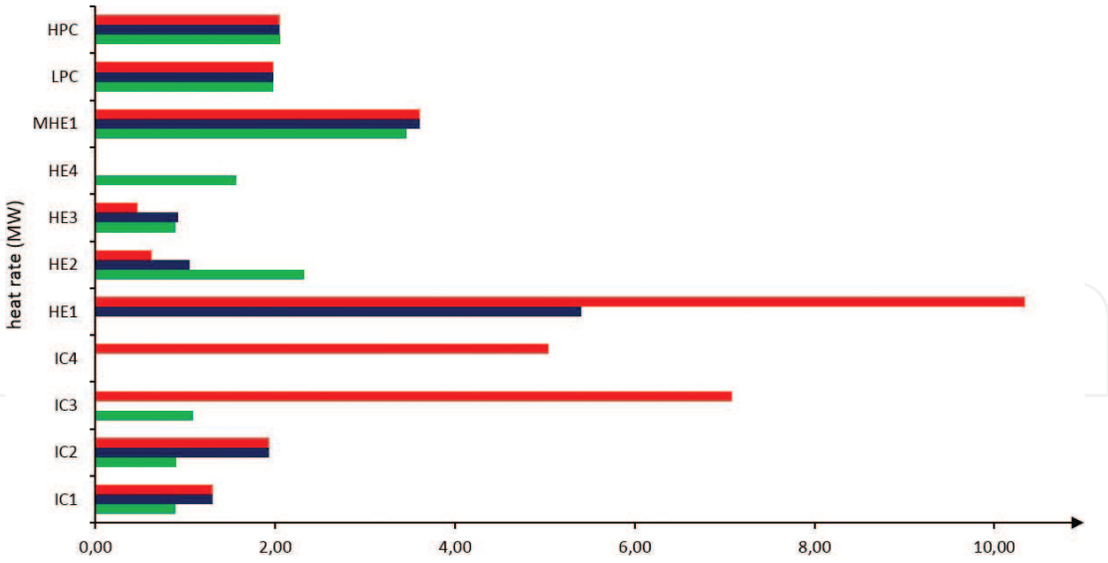

Figure 8. Heat rate within the heat exchangers (MW).

A decrease in the power consumption of more than 50%, if the regasification of LNG is introduced into an air separation process, has been reported in Refs. [20, 50]. Thus, the authors' results are in the range of the data reported by other scientists.

The results show that NC1 in Case A has the highest power consumption, followed by NC2 and NC5. In Case AD1, the power consumption of NC1 and NC2 is decreased by 50% (for each compressor). For Case AD2, the power consumption of the air compressors decreases as well due to the interstage cooling with LNG instead of water.

The heat rate in the heat exchangers varies significantly in the different systems. The HE1 in Case A is the component with the highest heat rate followed by the IC3 and IC4 in the nitrogen liquefaction block of the same system. The MHE has the same heat rate in Case A and AD1, because the air enters and leaves the MHE with the same temperatures. In Case AD2, the heat rate decreases slightly, because the air entering the MHE has a lower temperature. In addition, the heat rate in IC1 and IC2 is reduced from Case AD1 to Case AD2. In Cases A and AD1, the air is compressed within a two-stage compression process. In Case AD2, the air is compressed within a three-stage compression process, which decreases the temperature after each compressor, and, thus, results in a lower heat duty in the following interstage coolers.

5.2. Exergetic analysis

The definitions of the exergy of fuel and exergy of product for each component as well as for the overall systems are reported in Ref. [27]. The results of the overall system for Cases A, AD1, and AD2 are shown in **Table 3**. The exergetic efficiency increases form 34.7% in Case A to 42.2% in Case AD1 and to 54.1% in Case AD2. This corresponds to an increase in the exergetic efficiency by 21% from Case A to Case AD1 and an increase in the exergetic efficiency of 56% from Case A to Case AD2.

System	$\dot{E}_{F,tot}$, MW	$\dot{E}_{P,tot}$, MW	$\dot{E}_{D,tot}$, MW	$\dot{E}_{L,tot}$, MW	ε_{tot}, %
Case A	18.6	6.4	11.9	0.2	34.7
Case AD1	20.6	8.7	11.7	0.2	42.2
Case AD2	15.5	8.4	7.0	0.09	54.1

Table 3. Results obtained from the exergetic analysis of the overall systems.

Figures 9–11 show the exergy balances for all productive components of Cases A, AD1, and AD2, respectively. Each diagram has two axes: the left one is related to the exergy of fuel (MW) as the sum of exergy of product and exergy destruction, and the right one shows the exergetic efficiency (%).

The results obtained from the exergy analysis show that the exergetic efficiencies are around 90% for turbomachinery; however, for the heat exchangers, this value varies between 2% and 76%.

In Case A (**Figure 9**), the HE1 and the MHE are of particular interest. The HE1 is the component with the highest exergy destruction in this system. However, the component with the lowest exergetic efficiency is HE3. The exergetic efficiency of the MHE is 76%. This value is decreased in Case AD1 to 57% (**Figure 10**). In Case AD2, the IC1, IC2, and IC3 are productive components, but they have a very low exergetic efficiency between 2% and 7% (**Figure 11**). The air should not be cooled to the very low temperatures that are provided by LNG. It results in the low exergetic efficiency.

Figures 12–14 show the distribution of the exergy destruction among most important components for the Cases A, AD1, and AD2, respectively. The remaining components are lumped under "others."

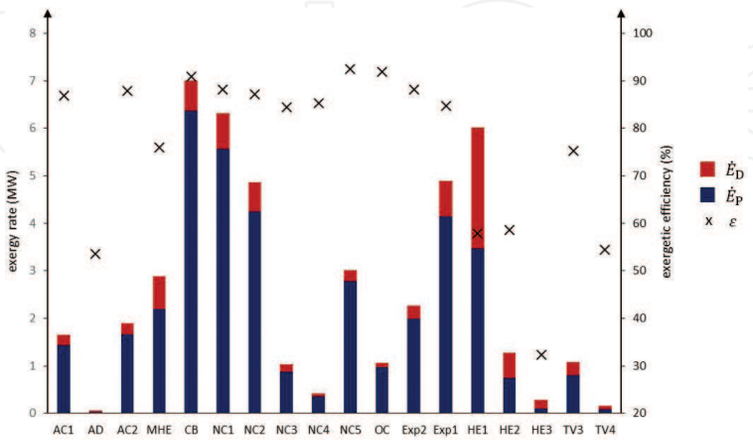

Figure 9. Results obtained from the exergy analysis of Case A.

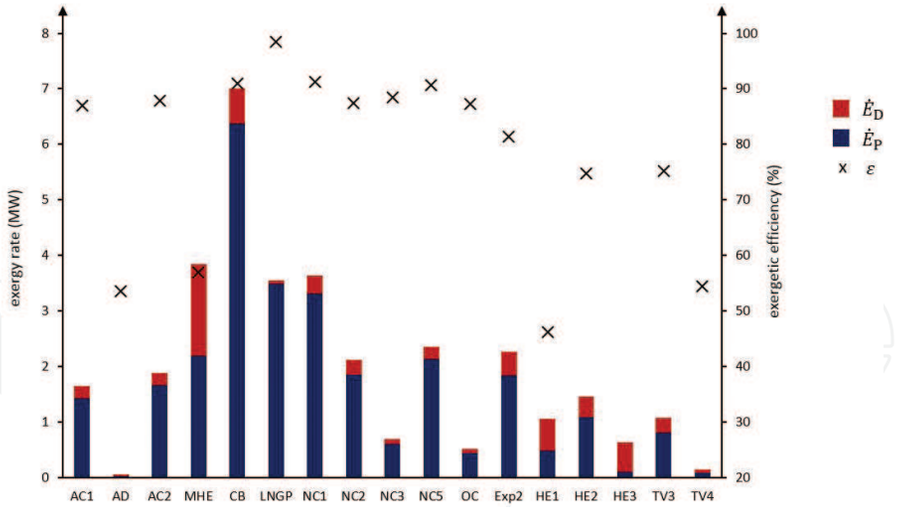

Figure 10. Results obtained from the exergy analysis of Case AD1.

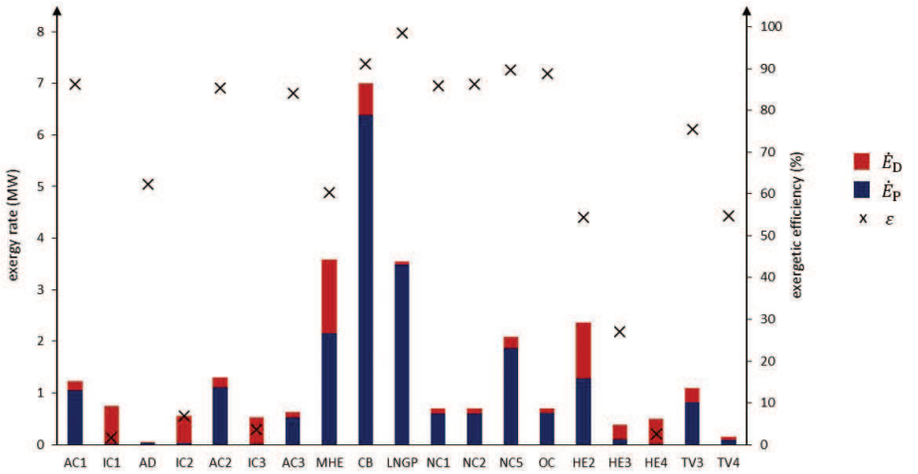

Figure 11. Results obtained from the exergy analysis of Case AD2.

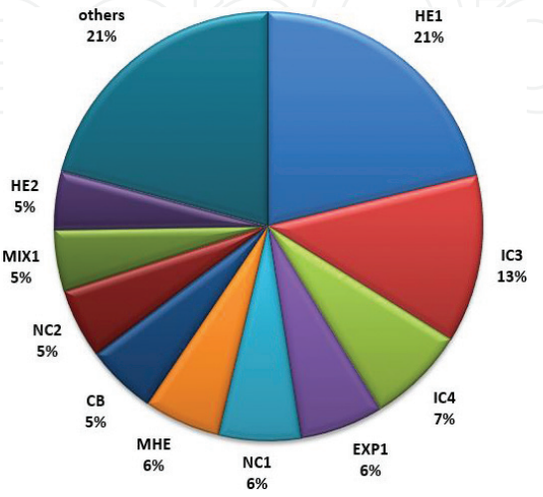

Figure 12. Distribution of the exergy destruction among components of Case A.

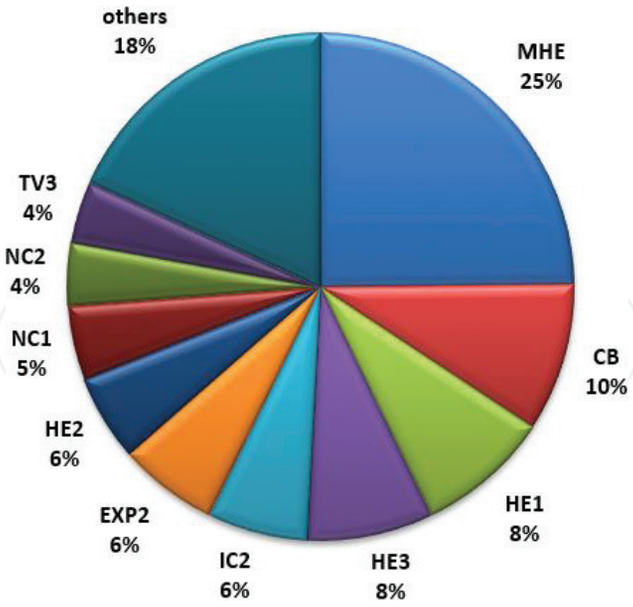

Figure 13. Distribution of the exergy destruction among components of Case AD1.

In Case A, HE1 is the component with the highest exergy destruction, which accounts for 21% of the total exergy destruction. The second component is the IC3 in the nitrogen liquefaction block with 13%. The structural changes from Case A to Case AD1 lead to a different priority. Hence, in Case AD1, the MHE is the component with the highest exergy destruction, i.e., 25% of the total exergy destruction. Of particular interest is also the CB with an exergy destruction of 10%. In Case A, however, both components (MHE and CD) play a minor role (around 5–6%). In Case AD2, the MHE is the component with the highest exergy destruction followed by HE2 and IC1. The contribution of the column block is only 9%.

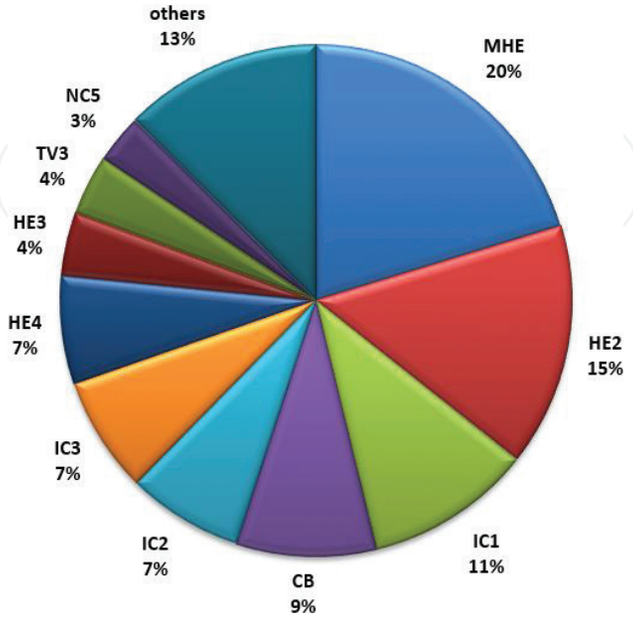

Figure 14. Distribution of the exergy destruction among components of Case AD2.

5.3. Advanced exergetic analysis

Figures 15–17 show the results obtained from the advanced exergetic analysis, for Cases A, AD1, and AD2, respectively. For all productive components, the exergy destruction is divided into unavoidable and avoidable exergy destructions.

The results obtained from the conventional exergetic analysis highlighted already that HE1 in Case A is the component with the highest exergy destruction, where approximately half of the exergy destruction could be avoided. The exergy destruction within HE3 is quite low, but it has a large potential for improvement, due to a relative high amount of avoidable exergy destruction.

In Case AD1, the MHE is the component with the highest exergy destruction, where just a small part could be avoided. The potetial for improvement is slightly higher for HE1 and HE2.

In Case AD2, the MHE and HE2 have the highest exery destruction with a relativ small potential for improvement. However, the components IC2 and IC3 could be improved.

5.4. Economic analysis

Figure 18 shows the estimated purchased equipment costs for three discussed cases. In addition to this information, the distribution of PEC among the group of components is demonstrated in **Figures 19–21**. The purchased equipment costs of the air compression and purification block and the column block are approximately the same for all three cases. However, the distribution within each case varies. While the share of the overall costs of the air compression and purification block differs slightly (between 7% and 9%), the share of the column block is affected more and varies between 40% and 54% for the three cases.

Table 4 shows the results of calculations of the fixed and total capital investment for the overall systems. The FCI and TCI of the Case AD1 is only slightly lower (3%) than the FCI and TCI of Case A. However, the difference between Case A and Case AD2 is far greater. Here, the FCI is 21.3% lower compared to Case A.

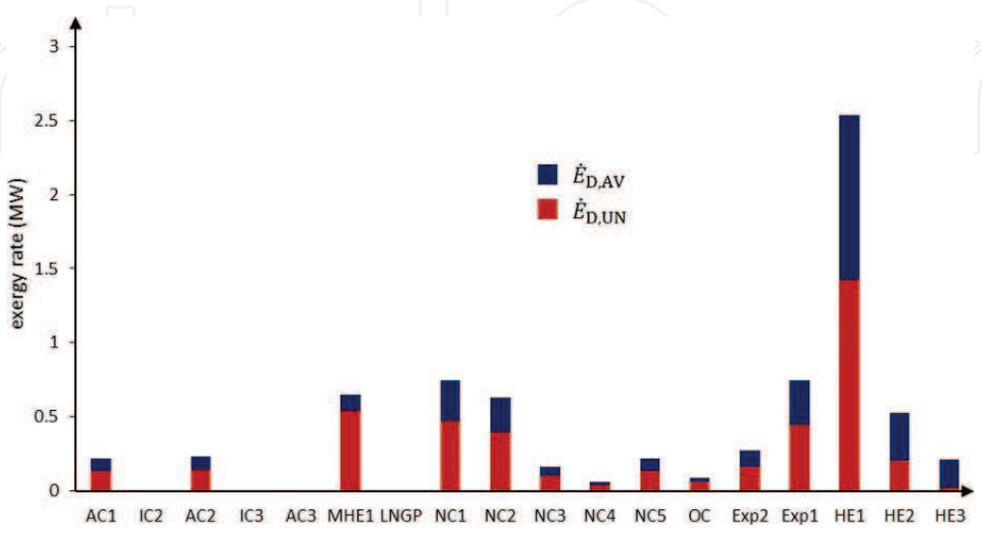

Figure 15. Results obtained from the advanced exergy analysis of Case A (MW).

http://dx.doi.org/10.5772/intechopen.70118

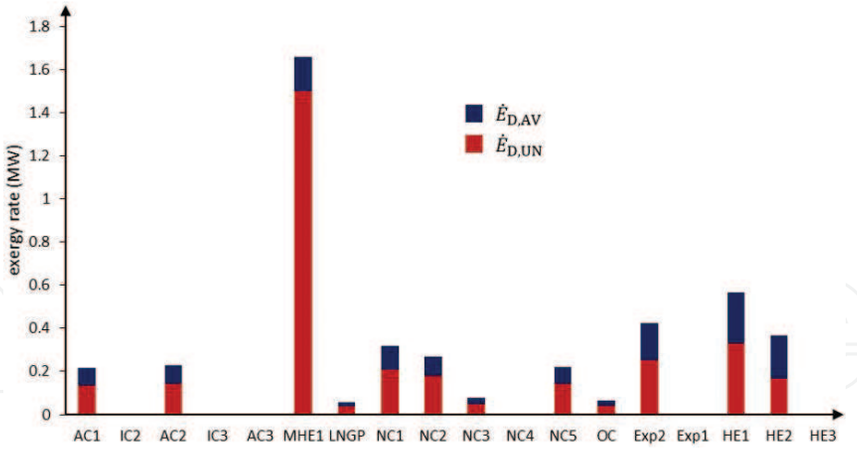

Figure 16. Results obtained from the advanced exergy analysis of Case AD1 (MW).

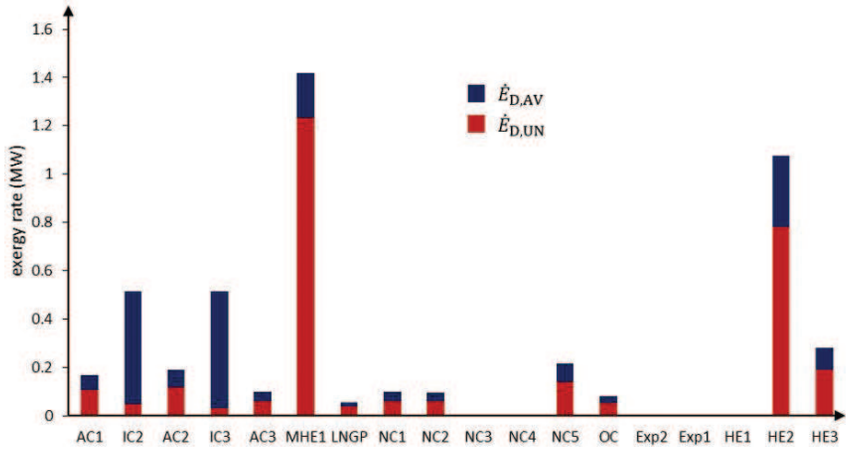

Figure 17. Results obtained from the advanced exergy analysis of Case AD2 (MW).

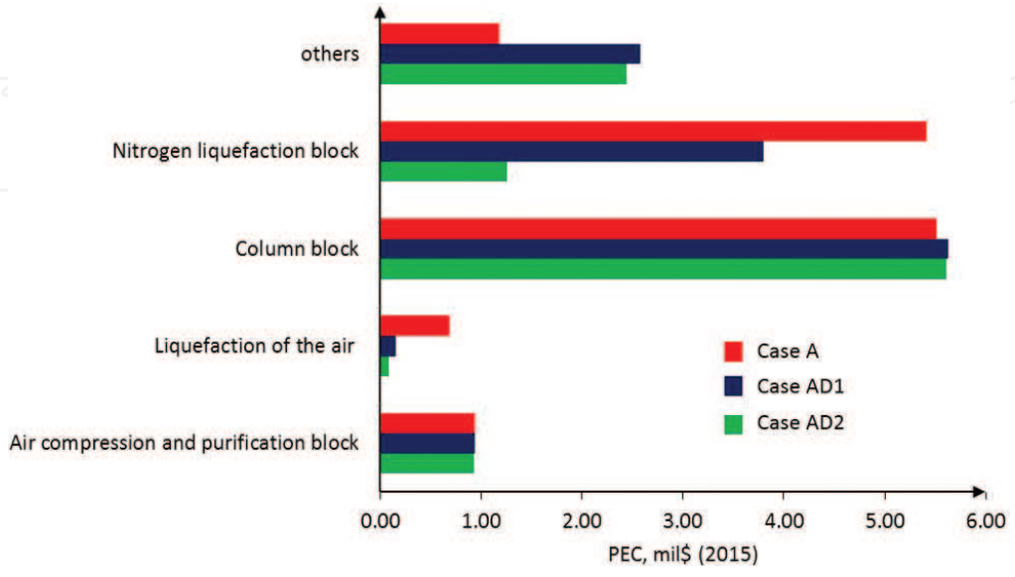

Figure 18. Purchased equipment costs for the Cases A, AD1, and AD2.

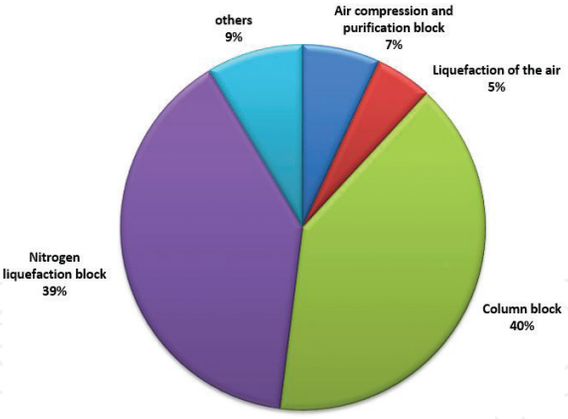

Figure 19. Distribution of the purchased equipment costs among the groups of components for Case A.

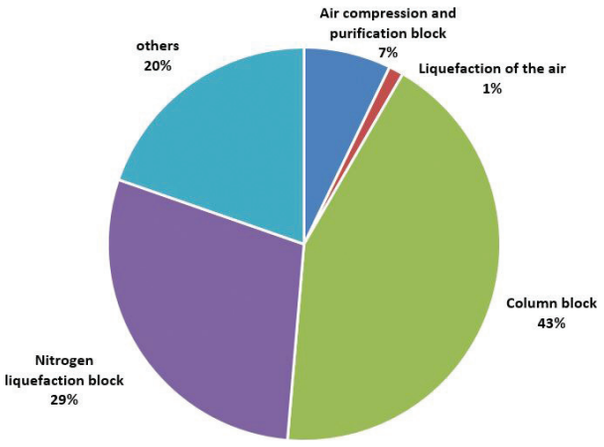

Figure 20. Distribution of the purchased equipment costs among the groups of components for Case AD1.

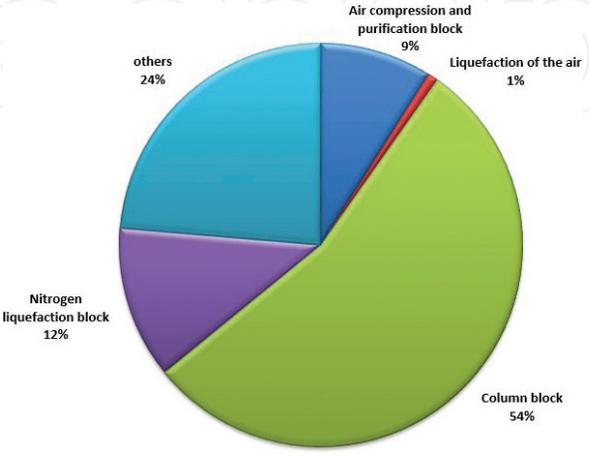

Figure 21. Distribution of the purchased equipment costs among the groups of components for Case AD2.

	Case A mil. US$ (2015)	Case AD1 mil. US$ (2015)	Case AD2 mil. US$ (2015)
Calculation of the fixed capital investment (FCI)			
Direct costs	41.4	39.9	32.6
Indirect costs	17.2	16.5	13.5
FCI	58.5	56.4	46.1
Calculation of the total capital investment (TCI)			
Plant facilities investment 1 (60% of FCI)	35.1	33.9	27.6
Plant facilities investment 2 (40% of FCI)	23.4	22.6	18.4
Interest for PFI 1 and PFI 2	9.7	9.4	7.6
TCI	68.2	65.8	53.7

Table 4. Results obtained from the economic analysis of the overall systems.

Unfortunately, the economic results cannot be compared with the data reported by other scientists because of the lack of such information in the literature.

6. Conclusions

In this chapter, the concept of the LNG-based industrial park is discussed. This means the integration of LNG regasification into different processes, where low temperatures are required in industrial plants. One option is the utilization of the low-temperature exergy of LNG during the liquefaction of air within an air separation unit. Exergy-based methods (conventional and advanced exergetic analyses) are applied to identify the potential for improvement of the discussed systems. The exergoeconomic and exergoenvironmental analyses will be reported later. The authors are also working on safety-related issues. A novel exergy-based method, the exergy-risk-hazard analysis, will be applied in order to identify the differences in the potential hazards for the proposed concepts.

Author details

Tatiana Morosuk[1]*, Stefanie Tesch[1] and George Tsatsaronis[2]

*Address all correspondence to: tetyana.morozyuk@tu-berlin.de

1 Exergy-Based Methods for Refrigeration Systems, Institute for Energy Engineering, Technische Universität Berlin, Germany

2 Energy Engineering and Environmental Protection, Institute for Energy Engineering, Technische Universität Berlin, Germany

References

[1] International Energy Agency. IEA: Key World Energy Statistics 2016. Available from: http://www.iea.org/publications/freepublications/publication/KeyWorld2016.pdf [Accessed: May 26, 2016]

[2] International Gas Union. IGU: World LNG Report 2016. Available from: http://www.igu.org/publications/2016-world-lng-report [Accessed: May 26, 2016]

[3] BP: Statistical Review of World Energy. 65th ed. Available from: https://www.bp.com/content/dam/bp/pdf/energy-economics/statistical-review-2016/bp-statistical-review-of-world-energy-2016-full-report.pdf [Accessed: February 28, 2017]

[4] International Group of Liquefied Natural Gas Importers. GIIGNL: The LNG Industry. 2016 ed. Available from: http://www.giignl.org/sites/default/files/PUBLIC_AREA/Publications/giignl_2016_annual_report.pdf [Accessed: May 26, 2016]

[5] Mokhatab S, Mak J, Valappil J, Wood D. Handbook of Liquefied Natural Gas. Amsterdam: Elsevier/Gulf Professional Publishing; 2013. ISBN: 9780124045859

[6] Yang CC, Huang Z. Lower emission LNG vaporization. LNG Journal. 2004;**11-12**:24-26

[7] Koku O, Perry S, Kim JK. Techno-economic evaluation for the heat integration of vaporization cold energy in natural gas processing. Applied Energy. 2014;**114**:250-261. DOI: 10.1016/j.apenergy.2013.09.066

[8] Angelino G. The use of liquid natural gas as a heat sink for power cycles. ASME Journal of Engineering and Power. 1978;**100**:160-177

[9] Morosuk T, Tsatsaronis G. LNG-based cogeneration systems: Evaluation using exergy-based analyses. In: Natural Gas—Extraction to End Use. InTech; 2012. pp. 235-266. DOI: 10.5772/51477

[10] Invernizzi CM, Iora P. The exploitation of the physical exergy of liquid natural gas by closed power thermodynamic cycles. An overview. Energy. 2016;**105**:2-15

[11] Xia G, Sun Q, Cao X, Wang J, Yu Y, Wang L. Thermodynamic analysis and optimization of a solar-powered transcritical CO_2 (carbon dioxide) power cycle for reverse osmosis desalination based on the recovery of cryogenic energy of LNG (liquefied natural gas). Energy. 2014;**66**:643-653. DOI: 10.1016/j.energy.2013.12.029

[12] Cao W, Beggs C, Mujtaba I. Theoretical approach of freeze seawater desalination on flake ice maker utilizing LNG cold energy. Desalination. 2015;**355**:22-32. DOI: 10.1016/j.desal.2014.09.034

[13] La Rocca V. Cold recovery during regasification of LNG part one: Cold utilization far from the regasification facility. Energy. 2010;**35**(5):2049-2058. DOI: 10.1016/j.energy.2010.01.022

[14] La Rocca V. Cold recovery during regasification of LNG part two: Applications in an agro food industry and a hypermarket. Energy. 2011;**36**(8):4897-4908. DOI: 10.1016/j.energy.2011.05.034

[15] Messineo A, Panno G. LNG cold energy use in agro-food industry. A case study in Sicily. Journal of Natural Gas Science and Engineering. 2011;**3**(1):356-363. DOI: 10.1016/j.jngse.2011.02.002

[16] Otsuka T. Evolution of an LNG terminal: Senboku terminal of Osaka gas. In: Proceedings of the 23rd World Gas Conference. Amsterdam, IGU (International Gas Union) 2006. pp. 1-14

[17] Yamanouchi N, Nagasawa H. Using LNG cold for air separation. Chemical Engineering Progress. 1979;**75**(7):78-82

[18] Nakaiwa M, Akiya T, Owa M, Tanaka Y. Evaluation of an energy supply system with air separation. Energy Conversion and Management. 1996;**37**(3):295-301. DOI: 10.1016/0196-8904(95)00787-3

[19] Jieyu Z, Yanzhong L, Guangpeng L, Biao S. Simulation of a novel single-column cryogenic air separation process using LNG cold energy. Physics Procedia. 2015;**67**:116-122. DOI: 10.1016/j.phpro.2015.06.021

[20] Mehrpooya M, Moftakhari Sharifzadeh M, Rosen M. Optimum design and exergy analysis of a novel cryogenic air separation process with LNG (liquefied natural gas) cold energy utilization. Energy. 2015;**90**:2047-2069. DOI: 10.1016/j.energy.2015.07.101

[21] Mehrpooya M, Kalhorzadeh M, Chahartaghi M. Investigation of novel integrated air separation processes, cold energy recovery of liquefied natural gas and carbon dioxide power cycle. Journal of Cleaner Production. 2016;**113**:411-425. DOI: 10.1016/j.jclepro.2015.12.058

[22] Agrawal R. Liquefied natural gas refrigeration transfer to a cryogenics air separation unit using high pressure nitrogen stream. US Patent No. 5,137,558 (August 11, 1992)

[23] Agrawal R, Ayres C. Production of liquid nitrogen using liquefied natural gas as sole refrigerant. US Patent No. 5,139,547A (August 18, 1992)

[24] Ogata S, Yamanoto Y. Process for liquefying and rectifying air. US Patent No. 4,192,662 (March 11, 1980)

[25] Perrotin G, Anselmini JP. Processes for the production of nitrogen and oxygen. US Patent No. 3,886,758 (June 3, 1975)

[26] Takagi H, Nagamura T. Method of using an external cold source in an air separation. European Patent No. 0304355 B1 (April 17, 1991)

[27] Tesch S, Morosuk T, Tsatsaronis G. Advanced exergy analysis applied to the process of regasification of LNG (liquefied natural gas) integrated into an air separation process. Energy. 2016;**117**:550-561. DOI: 10.1016/j.energy.2016.04.031

[28] Tesch S, Morosuk T, Tsatsaronis G. Exergetic and economic evaluation of safety-related concepts for the regasification of LNG integrated into an air separation processes. Energy. 2017. DOI: 10.1016/j.energy.2017.04.043 [in print]

[29] Cornelissen R, Hirs G. Exergy analysis of cryogenic air separation. Energy Conversion and Management. 1998;**39**(16-18):1821-1826. DOI: 10.1016/S0196-8904(98)00062-4

[30] Jain R, Piscataway N. Pre-purification of air for separation. US Patent No. 5,232,474A (August 3, 1993)

[31] Agrawal R, Herron DM. Air liquefaction: Distillation. In: Encyclopedia of Separation Science. Editor Wilson ID, Elsevier Science Ltd, Amsterdam, Netherlands: 2000. pp. 1895-1910. DOI: 10.1016/B0-12-226770-2/04821-3

[32] Bejan A, Tsatsaronis G, Moran M. Thermal Design and Optimization. New York: Wiley; 1996. ISBN: 978-047-1584-67-4

[33] Tsatsaronis G, Morosuk T. Understanding and improving energy conversion systems with the aid of exergy-based methods. Exergy. 2012;**11**(4):518-542

[34] Tsatsaronis G, Morosuk T. Understanding the formation of costs and environmental impacts using exergy-based methods. In: Energy Security and Development. The Global Context and Indian Perspectives. Editors. Reddy BS, Ulgiati S, New Delhi, India: Springer; 2015. pp. 271-292

[35] European Industrial Gases Association and Industriegaseverband. EIGA and IGV: Safe Practices Guide for Cryogenic Air Separation Plants. Available from: https://www.eiga.eu/fileadmin/docs_pubs/Doc_147_13_Safe_Practices_Guide_for_Cryogenic_Air_Separation_Plants.pdf [Accessed: December 16, 2016]

[36] Aspen Plus. The Software is a Proprietary Product of AspenTech, V8.6. 2014. Available from: http://www.aspentech.com

[37] Ulrich G, Vasudevan P. Chemical Engineering Process Design and Economics. A Practical Guide. 2nd ed. Durham, New Hampshire, US: Process Publishing; 2004

[38] Smith R. Chemical Process Design and Integration. Chichester, West Sussex, England: Wiley; 2005

[39] Peters M, Timmerhaus K, West R. Plant Design and Economics for Chemical Engineers. 5th ed. New York: McGraw-Hill; 2003

[40] Kerry F. Industrial Gas Handbook. Gas Separation and Purification. Boca Raton, Florida: CRC Press; 2007. ISBN: 9780849390050

[41] Häring HW. Industrial Gases Processing. Weinheim: Wiley; 2008. ISBN: 978-3-527-31685-4

[42] Ebrahimi A, Meratizaman M, Akbarpour Reyhani H, Pourali O, Amidpour M. Energetic, exergetic and economic assessment of oxygen production from two columns cryogenic air separation unit. Energy. 2015;**90**:1298-1316. DOI: 10.1016/j.energy.2015.06.083

[43] Bachmann C, Gerla J, Yang Q. Smaller is Better—New 3-in-1 Internals Reduce Air Separation Column Heights. Available from: https://www.sulzer.com/en/-/media/Documents/Cross_Division/STR/2013/STR_2013_3_16_19_Bachmann.pdf [Accessed: October 2, 2016]

[44] Epifanova V, Akselrod L. Air Separation Using Deep Cooling Methods: Technologies and Equipment. Moscow, USSR: Machinostroenie; 1976

[45] Guthrie KM, Grace WR. Data and techniques for preliminary capital cost estimating. Chemical Engineering. 1969:114-143

[46] Woodward JL, Pitblado R. LNG Risk Based Safety. Modeling and Consequence Analysis. Hoboken, New Jersey: John Wiley & Sons Inc. Publication; 2010. ISBN: 978-0-470-31764-8

[47] Pitblado RM, Baik J, Hughes GJ, Shaw SJ. Consequence of LNG marine incidents. In: Proceedings of the CCPS Conference; 29 June–1 July 2004; California Energy Commission, Orlando, USA. Available from: http://www.westernsunsystems.comorwww.gosolarcalifornia.org/lng/documents/CCPS_PAPER_PITBLADO.PDF [Accessed: April 6, 2017]

[48] Schmidt WI, Winegardner KS, DennehyI M, Castle-Smith H. Safe design and operation of a cryogenic air separation unit. Process Safety Progress. 2001;**20**(4):269-279

[49] Ramsden N, Roue R, Mo-Ajok B, Langerak G-J, Watkins S, Peeters R. Rahmenplan Flüssigerdags für Rhein-Main-Donau. 2015. Available from: https://www.portofrotterdam.com/de/file/5263/download?token=2wwYWvFk [Accessed: December 12, 2016]

[50] Sharratt C. LNG terminal cold energy integration opportunities offered by contractors. LNG Journal. 2012:22-24

[51] Kitagawa T. Survey of accidents at the air separation plants. The Journal of Ammonium Sulphate Engineering. 1964;**17**(3):47 [in Japanese, official translation by NASA Technical, Washington 1970]. Available from: https://archive.org/stream/nasa_techdoc_19710003182/19710003182_djvu.txt [Accessed: January 20, 2017]

IntechOpen